Journal of Nuclear Materials 406 (2010) 330–344

Contents lists available at ScienceDirect

Journal of Nuclear Materials

journal homepage: www.elsevier.com/locate/jnucmat

Microstructural evolution in the partial transient liquid phase diffusion bonding of Zircaloy-4 to stainless steel 321 using active titanium filler metal

M. Mazar Atabaki *

Department of Materials Engineering, Faculty of Mechanical Engineering, University Technology Malaysia, 81310, Malaysia
Institute for Materials Research, the School of Process, Environmental and Materials Engineering, Faculty of Engineering, University of Leeds, Leeds, UK

ARTICLE INFO

Article history:
Received 2 May 2010
Accepted 2 September 2010

ABSTRACT

Microstructural evolution of the partial transient liquid phase diffusion bonded Zircaloy-4 and stainless steel 321 using an active Ti-base interlayer were studied at different temperatures. Additionally, simple analytical models were developed to predict the evolution of the interlayer and intermetallics during the bonding operation. Bonds were characterized by scanning electron microscopy and energy dispersive X-ray spectrometry. Precision measurement of the interlayer width was made as a function of the bonding temperature. The liquid film migration occurred as a result of chemical solubility differences between the stable and metastable phases. The formation and growth model of the intermetallic compounds at the interfaces of Zircaloy-4/Ti-base interlayer and stainless steel 321/Ti-base interlayer for controlling the bonding process was studied considering the diffusion kinetics and the thermodynamics. The evolution of the interlayer thickness indicated a good agreement between the calculation and experimental measurement. It was also demonstrated that the low isothermal solidification kinetic was not only due to the enrichment of the liquid phase with the base alloying elements such as Ti and Zr, but also the reduction of solid solubility limit of Cu in the base alloys contributed to the reduction of isothermal solidification kinetic.

1. Introduction

Zirconium-based dissolver vessels containing highly radioactive and concentrated corrosive nitric acid solution needs to be joined to the rest of fuel reprocessing plant made of stainless steel [1–3]. Zr alloys have superior thermal properties compared to other traditional materials in consideration for spent nuclear fuel containers [2]. Solid-state joining process like friction welding was applied to join Zircaloy-4 and type 304L stainless steel. This welding process produces brittle intermetallics at the interface and showed a huge reduce in the mechanical strength as well as the corrosion resistance of the joints [4–6]. Hairong et al. [7] studied the microstructure of explosive welded joints between Zircaloy-4 and stainless steel and observed a crystalline phase $Zr(Fe, Cr)_2$ with hexagonal structure. The brittleness of the Zr alloy and steel bonds is generally due to the formation of intermetallic compounds. Such formation is very serious when fusion occurs, as in arc-welding. In order to avoid the formation of intermetallic compounds several processes have been developed [8–11].

Scientists have used Fe, Pt, Ti and Ta interlayers to optimize the bond properties by utilizing the diffusion bonding [12–15]. However, there exist a hybrid joining process named transient liquid phase diffusion bonding in which the formation of the deleterious phases can be prevented. For a given bonding temperature, transient liquid phase diffusion bonding relies on the time required to complete the isothermal solidification to prevent the formation of the brittle eutectic phases in the joints [16]. Although transient liquid phase bonding is a reliable bonding technique, the time required to complete isothermal solidification is long enough to allow the intermetallics grow within the joint area. Therefore, in some cases it is needed to decrease the solidification time by partial transient liquid phase diffusion bonding method [17]. Partial transient liquid phase joints are formed when a melting point depressant in the interlayer diffuses into the parent alloys and incomplete isothermal solidification results. One of the critical aspects for the bonding process is the selection of the interlayer. For instance, in the certain engineering applications, such as the repair of nuclear power plant parts, boron containing interlayers cannot be used. This is due to the very large neutron absorption cross-section when materials containing boron are used, which results in reduced nuclear reactor performance. Additionally, boron can transmute to helium due to radiation induced porosity, risk of material swelling and, as a result, may cause brittleness of structural materials [18].

* Corresponding author. Address: Materials Engineering Department, Faculty of Mechanical Engineering, University Technology Malaysia, Skudai, Johor Bahru 81310, Malaysia. Tel.: +60 17 7820742.
E-mail address: m.mazaratabaki@gmail.com

0022-3115/$ - see front matter © 2010 Elsevier B.V. All rights reserved.
doi:10.1016/j.jnucmat.2010.09.003

The major reasons for using partial transient liquid phase diffusion bonding in this study are as follows. Firstly, since no melting or additional materials are involved, there is no discontinuity in the microstructure and therefore no discontinuity in properties at the bond. Secondly, since a pressure required to form the bond is very low with respect to the yield strength of the materials, there is no distortion of the couples during the bonding, nor are any temperature gradient developed. Thirdly, the prevention and control of the formation of intermetallic compounds can be achieved through a control on partial diffusion of elements in both sides of the joint.

This study concentrates on an approach to joint Zircaloy-4 and stainless steel (grade AISI 321) by partial transient liquid phase diffusion bonding using an amorphous titanium interlayer with 40 μm thickness. Along with the experimental results a model is introduced to comprehensively determine the thickness of the interlayer and the kinetics of forming the intermetallics during the bonding operation. Experimental results are compared to predictions for isothermal solidification given by a selection of analytical and numerical models.

2. Experimental procedure

The nominal compositions of the alloys and interlayer chemical composition are shown in Table 1. The choice of an active metal like Ti-base alloy provides excellent compatibility with Zr, due to partial solid solubility in the β range into each other. The filler metal is compatible with stainless steel, as it forms solid solution and intermetallic compounds, due to the migration of alloying elements. Presenting Zr in the filler metal helps to increase the compatibility of the interlayer to both sides of the joint. Specimens of 4 mm width and 10 mm length to 10 mm height were prepared by cutting from stainless steel 321 and Zircaloy-4. Specimens were polished down to 0.30 μm on lapping machine using diamond paste. After polishing, the specimens were ultrasonically cleaned for about 15 min in a solution of acetone. Subsequent to this, the filler alloy was placed between the mating surfaces of the cleaned couples, and the assembled specimens fitted up by a fixture made by Zircalloy-4 to prevent any expansion during the bonding operation.

The partial transient liquid phase diffusion bonding was accomplished in a vacuum furnace equipped with a hydraulic press. For diffusion couple preparation, Zircaloy-4, Ti-base interlayer and stainless steel 321 were pressed against each other at the polished surfaces, utilizing a compression assembly. The assembly containing the diffusion couple was introduced into a tube furnace under a vacuum of 5×10^{-6} Torr. The couples were then heated at a rate of 20 °C/min until the diffusion temperature was attained. After annealing, the couples were cooled quickly by a blast of cold argon. A range of optimum temperatures, 1123 and 1223 K, was set as diffusion temperatures for 20 min holding time. The bonding regimes were as follows: heating to diffusion temperature at a rate of 20 °C/min; soaking for 20 min; putting 1 MPa pressure on the specimen; cooling at a rate of 20 °C/min.

The marked regions of the polished and unetched diffusion couples of Zircaloy-4/Ti-base interlayer/stainless steel 321 at different temperatures were analysed with the electron probe micro-analysis operating at beam energy of 15 keV with a stabilised beam current of 100 nA. The specimens were loaded in the microprobe such that the diffusion interface was perpendicular to *X*-axis of the specimen stage and hence parallel to the electron beam. Specimens of the joint cross-section were prepared by a common metallographic procedure using Buehler Phoenix Beta grinder–polisher.

Considering the microstructural observations, a model is derived to describe the evolution of the interlayer during partial transient liquid phase diffusion bonding of Zircaloy-4 to stainless steel 321. In this model growth of the interlayer during bonding operation is explained. In addition, the effect of the bonding temperature and the bonding time on the thickness of the interlayer was analysed numerically using Fick's second law. Moreover, the direct effects of the intermetallics on the joint's properties are discussed considering the kinetics of the nucleation and growth of the intermetallic compounds during the bonding process.

3. Results and discussion

3.1. Microstructure of the bonded specimens

A typical micrograph of the diffusion zone for the assembly bonded at 1123 and 1223 K for 20 min depicting several interfaces is shown in Fig. 1. Microstructure examination of the diffusion zone indicates that it contains two small regions: a region having light contrast near the stainless steel 321 side and a region having a dark contrast near the Zircaloy-4 side. The thickness of each of two regions increased with increasing the diffusion temperature and the initial thickness of the interlayer decreased with increasing the diffusion temperature (shown in Table 2). The phase was in the form of islands extending over most of the diffusion zone. The insert layer elements spread through both sides and some elements preponderated in the diffusion zone. Comparing the results obtained by metallography showed that the dark region represents the solid solution phases, while the light region represents the ferrous phases. The structure of the diffusion zone formed at 1123 K for 20 min indicates that diffusion occurred incompletely. The normal α-Zr structure is retained adjacent to the interface at regions which diffusion did not happen through the bonding operation. The interesting thing is that neither Zircaloy-4/Ti-base interlayer side nor stainless steel 321/Ti-base interlayer side contains any defects like cracks and voids.

The thickness of the diffusion zone, determined in the bonded regions, increased slowly with temperature. For instance, at 1123 K the thickness of Zircaoly-4/Ti-base interlayer was 8 μm at diffusion time of 20 min, while the thickness of stainless steel 321/Ti-base interlayer in the same condition was 4 μm. This fact can be attributed to the closer liquidus temperature of the interlayer and Zr alloy that are more convenient to move from one side to other side. The grain appears to have a columnar structure, indicative of localized melting and solidification. As shown in Fig. 1b, very fine precipitates at the grain boundaries formed as a result of higher temperature. It is also noted that some elements penetrate into large distances far beyond the diffusion zone and the zone of grain growth in Zircaloy-4 side. It is clear by increasing the bonding temperature coarse grain structure resulted from

Table 1
Chemical compositions of materials (wt.%).

Alloy type	Element composition (wt.%)								
	Cr	Sn	Ni	Cu	Mn	C	Fe	Zr	Ti
Stainless steel 321	18	–	9.5	–	2	0.08	Bal.	–	0.8
Zircaloy-4	0.10	1.52	<0.005	–	–	0.002	0.20	Bal.	–
Ti interlayer	–	–	15	17	–	–	–	23	Bal.

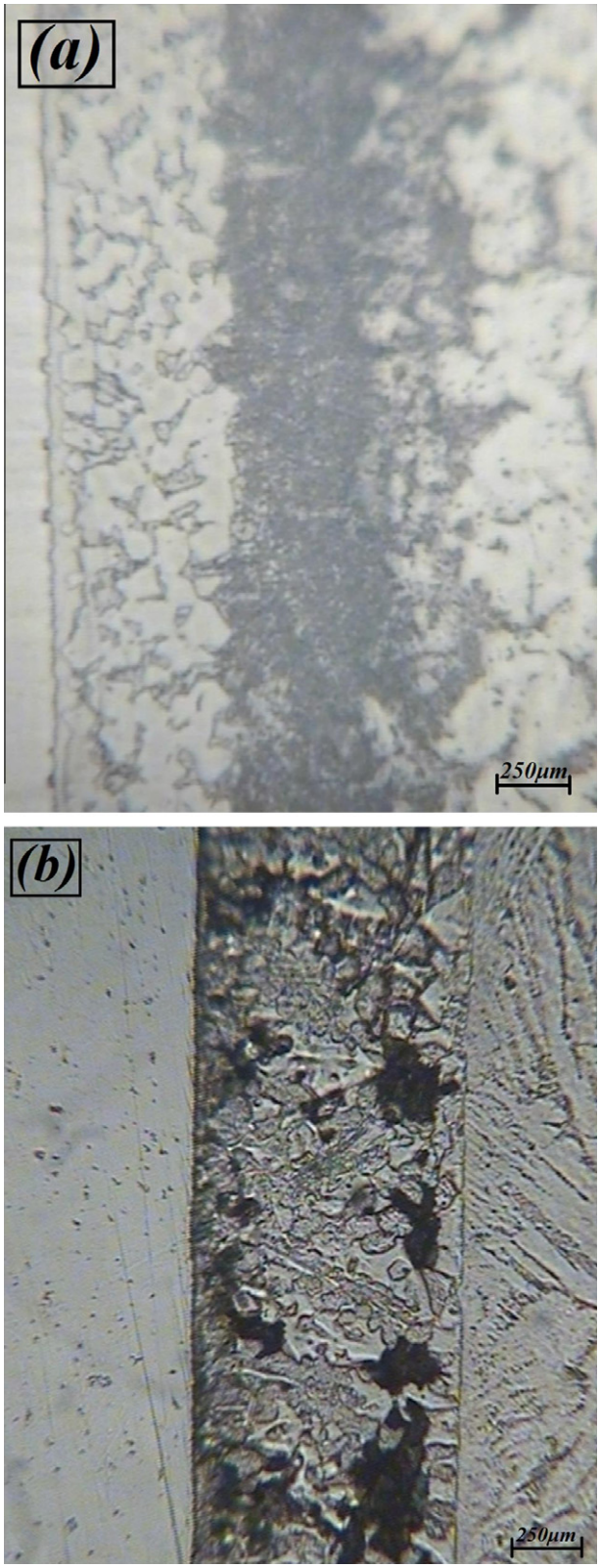

Fig. 1. Microstructure of the cross section of the partial transient liquid phase diffusion bonded specimens at two temperatures; (a) 1123 K and (b) 1223 K for 20 min (see Widmanstätten structure at the right side of the joint).

diffusional growth by recrystallization of the steel substrate. This coarse structure changed at the higher temperature to a columnar structure (Fig. 1a and b). On the other hand, the Zr substrate shows excessive grain growth after recrystallization and phase transformation at the higher bonding temperature.

Observation with SEM revealed that several interaction layers were formed in the diffusion area with different chemical analyses as shown in Fig. 2 and Table 3. At bonding temperature of 1223 K, the Zr substrate showed no evidence of diffusion since the analysis of regions *B* and *C* in Fig. 2 showed a large amount of Zr was diffused from the Zircaloy-4 side to the interlayer area close to the Zr substrate. The ratios between Ti, Cu, Zr, Fe, and Cr are close to CuTi, Cu_2Ti, $ZrFe_3$, $ZrFe_2$ and $Zr(Cr, Fe)_2$. From Table 3 it was clear that the Zr of the interlayer severely diffuses beyond the diffusion zone. It is found that cooling the specimens before the isothermal solidification completion results in formation of the non-isothermal solidified phases such as intermetallic and eutectic constituents in the bonding zone (see Figs. 1 and 2). The non-isothermal solidification in the bonding area results in the enrichment of the residual liquid phase with the positive segregating alloying elements ($K_i < 1$, K_i is solute distribution coefficient of element i) and remaining of the melting point depressant elements in this phase. These factors cause formation of deleterious phases in the bonding zone. However, it is suggested that considerable diffusion of Ti and Zr from the base alloys to the liquid phase occurred by increasing the bonding temperature. High diffusivity of the alloying elements at the higher temperature, according to the Arrhenius equation, and steep concentration gradient between the liquid and the solid phase (Fig. 3) results in the enrichment of the liquid phase with the base alloying elements. Moreover, increase in the bonding temperature, higher than the eutectic temperature of Ti–Zr, raises the diffusivity of Ti but noticeably reduces the solid solubility of Ti in the base metal.

According to the Zircaloy-4 phase diagram, increasing the bonding temperature causes a phase transformation. Zr in solid state undergoes an allotropic transformation from the low temperature hexagonal closed-packed (hcp) α-phase to body-centred cubic (bcc) β-phase at 1138 K [18]. Solid state phase equilibria of Zircaloy-4 have been investigated experimentally by Miquet et al. [19], who reported a prevalence of four phase domains: $\alpha + \chi$ up to 1081 K, $\alpha + \beta + \chi$ from 1081 to 1118 K, $\alpha + \beta$ between 1118 and 1281 K, and β-phase above 1118 K. Here, χ refers to the intermetallic hexagonal Laves phase $Zr(Fe, Cr)_2$ [20]. Quenching Zircaloy from β-phase in moderate cooling rates produces two variants of Widmanstätten structure, namely, the basketweave and the parallel-plate structure [21]. Based on the results of the present study at 1123 K, $\alpha + \beta$ phase is formed at the Zircaloy-4 side (Fig. 1a) and fine grains were observed. On the other hand, at 1223 K of bonding temperature Widmanstätten structure was observed (Fig. 1b) at the Zircaloy-4 side and the hexagonal lave phase $Zr(Fe, Cr)_2$ was formed in the bonding area. It is believed that using the Ti content filler metal accelerated the phase transformation both at the grain boundaries and in the bulk metal and this lead forming higher Widmanstätten structure at the contact area to the filler alloy. Therefore, a large amount of coarse acicular Widmanstätten structure formed in the Zircaloy-4/Ti-base interlayer side, because the bonding temperature exceeds the β-transus temperature of Zircaloy-4. From another stand point, presenting Cu and Ni raised the temperature of phase reactions, causing intergranular nucleation to occur earlier and intragranular nucleation to occur later at the mating surface of Zircaloy-4 and Ti-base interlayer.

The concentration of Ni in the vicinity of the stainless steel side of the boundary becomes very low compared to that of Cr. These conditions are conductive to the formation of regions containing some ferritic phase at room temperature depending on local concentration of Ni, Cr and Fe, in these regions. Fe and Ni form eutectics with Zr at temperatures of 1123 K and 1223 K, respectively, which are below the melting point of either the Zircaloy-4 or the stainless steel (see Fig. 6d and e). Thus some eutectic melting on

Table 2
Thickness of different regions of the diffusion zone for samples joined at different temperatures.

Diffusion temperature		Thickness of the diffusion zone (μm)			Thickness of the interlayer (μm)
T	K (°C)	Total	Zircaloy-4 side	Stainless steel 321 side	
T_1	1123 (850)	10	8	2	30 ± 0.8
T_2	1223 (950)	23	19	4	17 ± 0.3

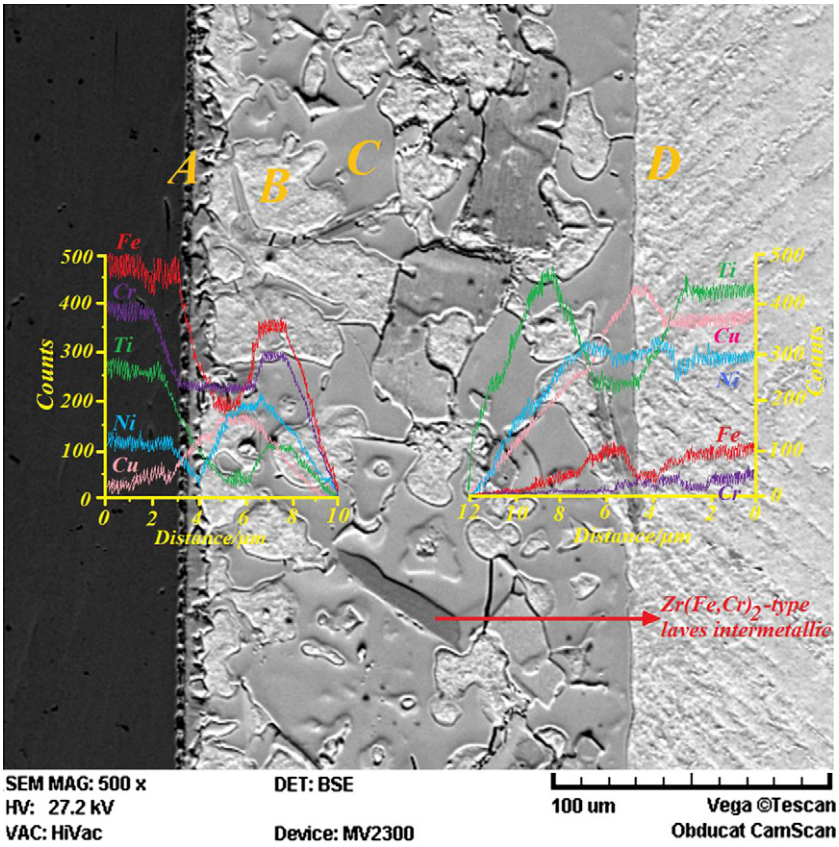

Fig. 2. SEM micrograph of Zircaloy-4/Ti-base interlayer/stainless steel joint bonded at 1223 K showing partial diffusion and incomplete isothermal solidification.

Table 3
Chemical analyses at points shown in Fig. 2.

Symbol	Average chemical analyses (wt.%)					
	Fe	Cr	Ni	Ti	Cu	Zr
A	24.1	20	1.2	9.8	0.4	Bal.
B	1.5	0.3	0.6	4.5	1.4	Bal.
C	14.1	2	5.4	8.3	3	Bal.
D	1	–	0.4	2.5	–	Bal.

the Zircaloy-4 side with consequent columnar grain growth occurred in the region adjacent to the diffusion zone where the concentration of Fe and Ni are expected to be high enough to form eutectics. Moreover, the accumulation of Cr to the near interface of Zircaloy-4/Ti-base interlayer makes diffusion barrier for Ti. Fig. 4 shows the junctions which are obtained at 1123 K, between Zircaloy-4, Ti-base interlayer and stainless steel. The interface shows various phases formed by the chemical elements (Table 4), of four regions. The point is that the thickness of the diffusion zone in both sides considerably increased since the temperature of bonding increased to 1223 K, especially in the Zircalloy-4 side the diffusion zone thickness 2.5-fold enlarged. The main reason of the larger diffusion zone is related to the difference in the acti-

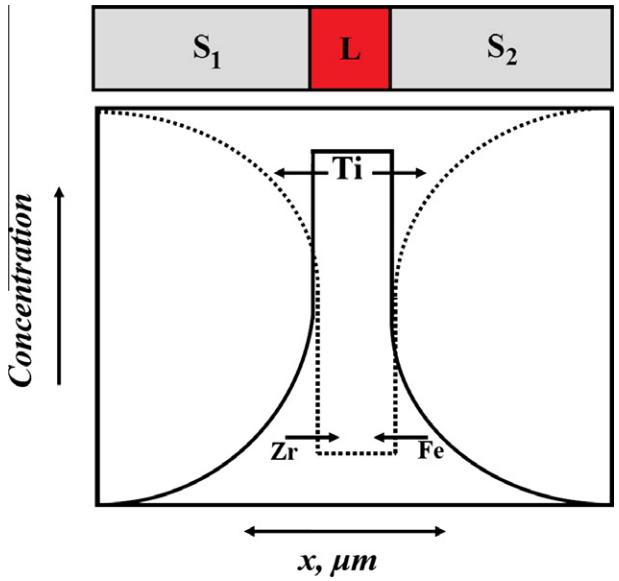

Fig. 3. Interdiffusion between the solid and liquid phases; arrows indicate the direction of diffusion of the alloying elements.

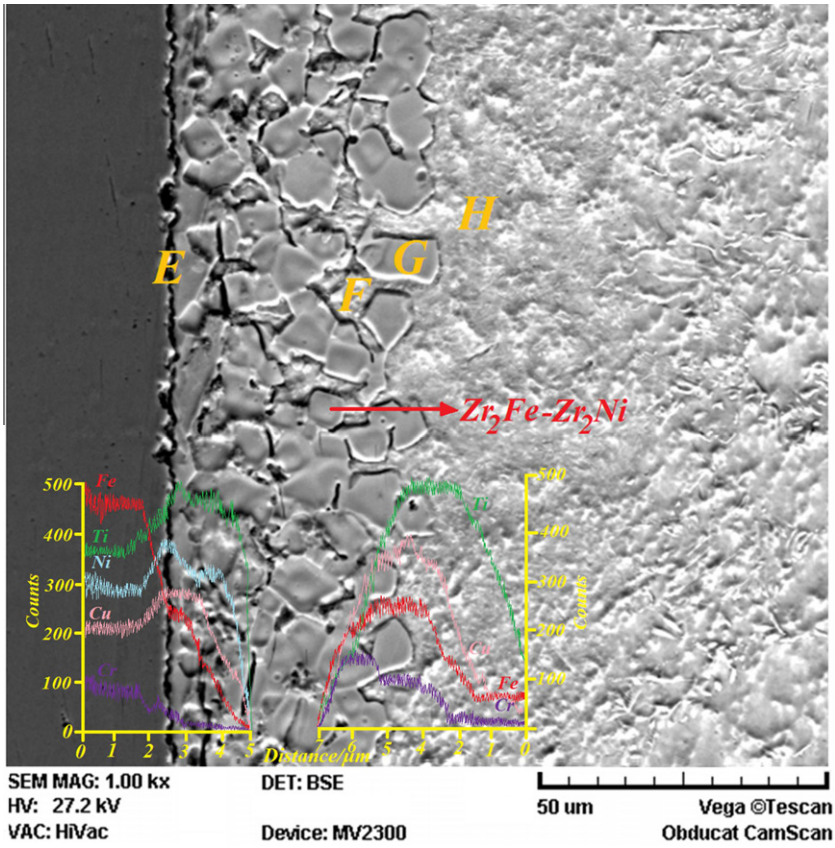

Fig. 4. SEM micrograph of Zircaloy-4/Ti-base interlayer/stainless steel joint bonded at 1123 K showing partial diffusion and very small values of isothermal solidification.

Table 4
Chemical analyses at points shown in Fig. 4.

Symbol	Average chemical analyses (wt.%)					
	Fe	Cr	Ni	Ti	Cu	Zr
E	7.2	2.6	12.3	22.6	19.8	Bal.
F	2.6	0.6	13.3	9.2	21.2	Bal.
G	4.8	0.8	12.7	22.7	16.4	Bal.
H	0.2	–	0.7	16.7	1.8	Bal.

vation energies required for the reaction, which are 90.07 and 35.4 kcal/mol for Fe–Ti and Zr–Ti [15], respectively. The intermetallic compounds containing Zr, Fe, Cr and Ni are not present in a compact layer near the Zircalloy-4 side. Apparently these elements before the formation of FeCr and $Zr(Fe, Cr)_2$ were diffused. At temperature of 1123 K, the concentration of Fe was very high, compared with that of Zr in the stainless steel 321 side. As can be seen from Table 4 the Fe concentration altered dramatically in the area *F* as a result of forming a eutectic.

As shown in Fig. 5, Zr forms almost ideal solutions with Ti in both liquid and solid states, whereas the solubility of Zr in Cr at 1123 K is almost zero. Therefore, at the beginning of the bonding, Ti as a main element in the initial molten filler would at first react more actively with the Zr rather than with Cu to cause an intensive dissolution of the Zr base metal. Due to this different reactivity of Zr with the Ti-base interlayer, the molten liquid becomes rich in Zr at the initial stage of the bonding. Due to this enhanced reaction with the Ti-rich molten liquid, an inward diffusion of the Zr base metal was promoted considerably, so the content of Zr gradually increased in the joint. In these mechanisms, the overall composition of the joint changed from Ti-rich to (Zr, Ti)-rich and finally into Zr-rich by increasing the bonding temperature (see Fig. 6a–f). As indicated in Tables 3 and 4, the phases formed in all the joints are mostly Ti–Zr-based compounds, which are stable not only at room temperature but also at 1123 K [22,23]. So it was expected that the formation of these phases was closely related with an isothermal solidification and a subsequent solid-state interdiffusion between the base metals and molten liquid during the isothermal

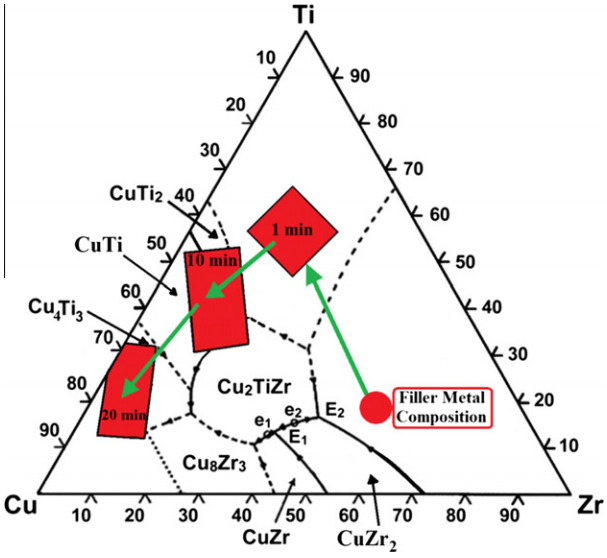

Fig. 5. Compositional change of the main phases in the joint.

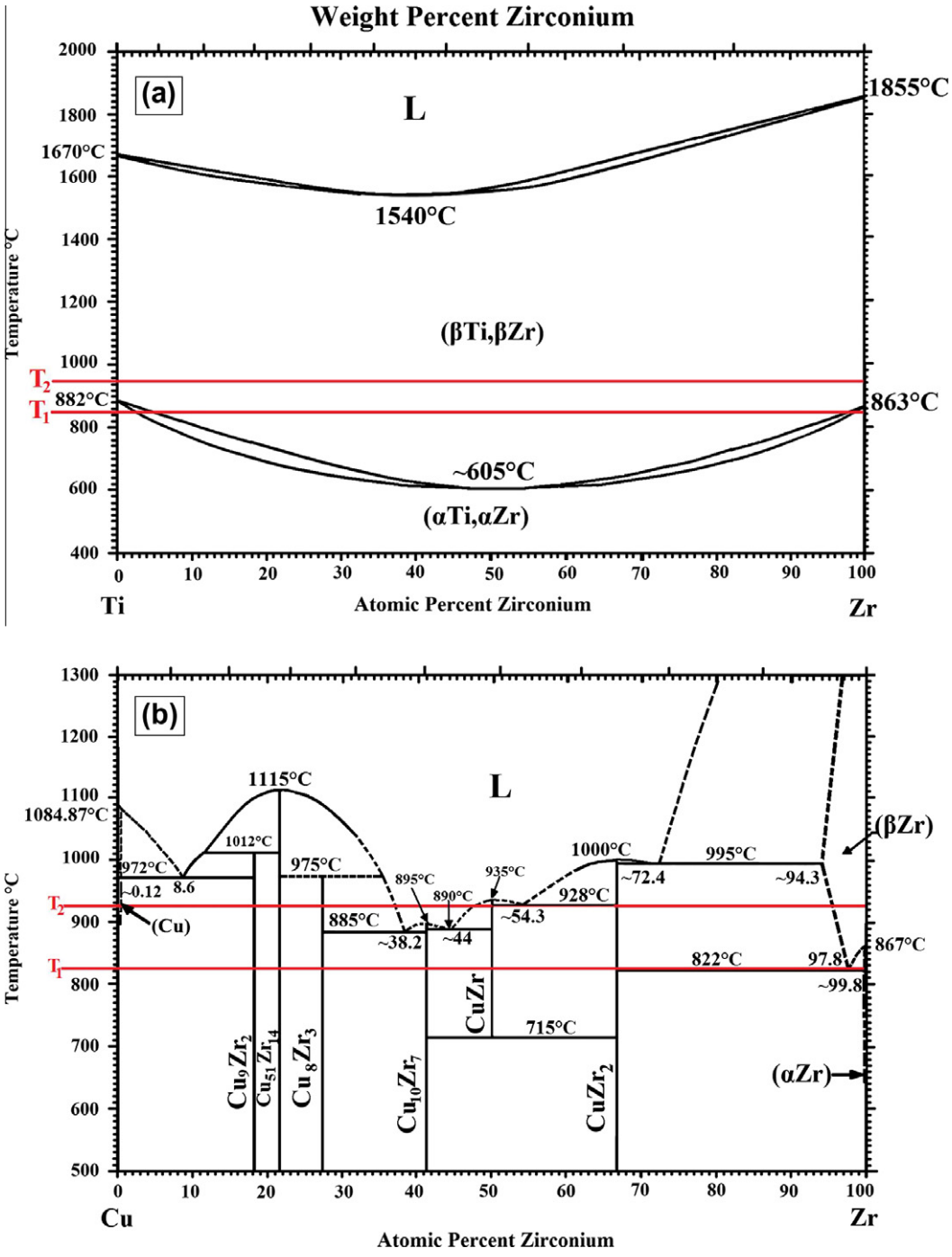

Fig. 6. Binary alloy phase diagrams: (a) Ti–Zr, (b) Cu–Zr, (c) Ti–Cu, (d) Zr–Fe, (e) Ni–Zr and (f) Ti–Fe.

holding at the bonding temperature. Based on the equilibrium Ti–Cu binary and Ti–Zr–Cu ternary alloy phase diagrams, the Cu_2Ti phase cannot be observed at room temperature and should transform to other phases during the cooling.

Nonetheless, it is believed that increasing isothermal-solidification rate caused by the higher diffusivity with increasing the bonding temperature [29]. Moreover, presence of the second phase particles within the base alloy at the joint-substrate interface slow down the solidification process resulting in increasing the time required to prevent the formation of eutectic-type microconstituents at the joint [40]. Based on the Ti–Zr and Ti–Fe diagrams (Fig. 6a and f), liquidus concentration reduces with increasing the bonding temperature, which implies that for the initial filler alloy composition close to the eutectic value, more base material required to melt back into the liquated filler in order to dilute the liquid to attain equilibrium composition. As it was observed, the eutectic was formed from residual liquated insert during cooling from the bonding temperature due to insufficient diffusion of the solute, Ti, away from the liquid to achieve complete isothermal solidification during the holding time.

It should be pointed out that diffusion of carbon from the stainless steel side to the Ti-base interlayer occurs at both bonding temperatures as a result of interstitial interdiffusion of carbon in the Ti-base interlayer structure but the effect of that parameter in the microstructural evolution of the bonded couple was not studied in the present investigation.

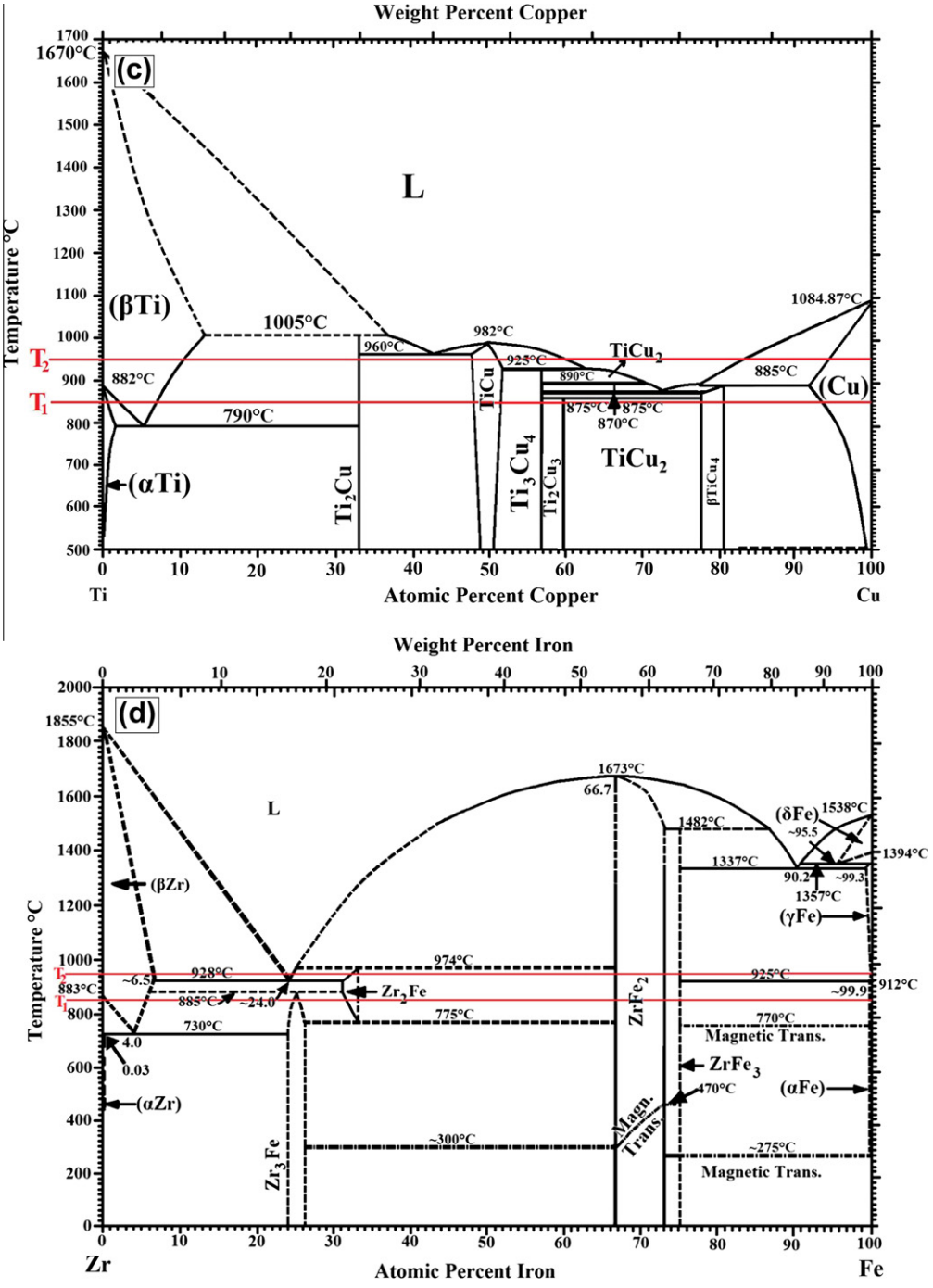

Fig. 6 (*continued*)

3.2. Modelling of partial transient liquid phase bonding for Zircaloy-4/Ti-base alloy interlayer/stainless steel 321 couple

Considering the reaction products and the evolution of the eutectic phases in the bond region, it is more precise to predict the evolution of the interlayer thickness during bonding operation. However, the development of the phases was specifically surveyed in other researches [12,15,24]. The critical requirement in the partial transient liquid phase diffusion bonding is that the liquidus temperature of the alloys varies with composition. It is then possible for the variation in composition of the inhomogeneous alloys to cause localised melting at the bonding temperatures where the mass of material remains solid. The transience of the liquid phase, and its trace in the solid, arises from changes in composition as a result of diffusion. In the following model the widening of the interlayer between liquid and solid is described.

3.2.1. Effect of bonding temperature

Mathematical modelling coupled with experimental data is widely used to determine the transient liquid phase bonding kinetic parameters [25–27]. These models are mostly based on the use of pseudo-binary phase relationships between liquid interlayer and solid base alloy, and depend on classic solutions to Fick's laws of diffusion. According to these models, an increase in bonding temperature is expected to increase isothermal-solidification rate, and produce a eutectic-free joint in a reduced time, $t_{f(\text{holding time})}$,

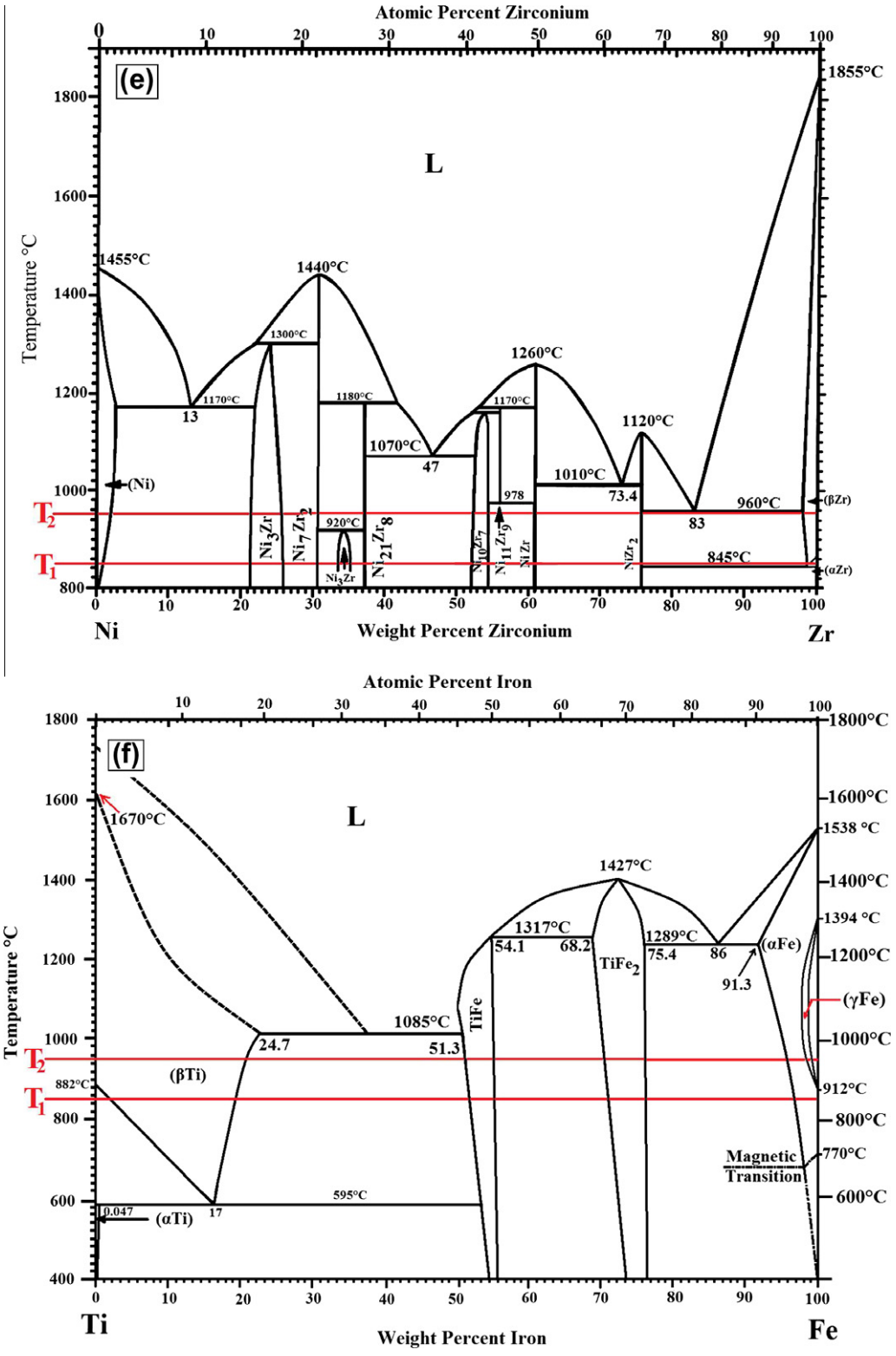

Fig. 6 (*continued*)

compared to the time needed at lower temperatures. However, an increase in bonding temperature may not necessarily result in a faster solidification process, as the actual rate of solidification will depend upon details of the phase relationships in complex alloy and on diffusivities of solutes across the solid–liquid interface. Sinclair et al. [28,29] suggested that deviation from isothermal-solidification rate predicted by conventional transient liquid phase bonding diffusion models, which are generally based on binary phase relationships, might be encountered during transient liquid phase bonding of multi-component systems. It was proposed that if the solubilities or diffusivities of the two diffusing solutes capable of controlling the isothermal solidification process are very

different, the isothermal solidification stage could be divided into two parabolic regimes; the faster solute and the slower solute.

In the present work, diffusion of Ti, which has high diffusivity compared to substitutional solutes, is believed to be isothermal-solidification rate controlling factor during the bonding at 1123 and 1223 K. Thus, an increased diffusivity of Ti with an increase in bonding temperature from 1123 K to 1223 K results a reduction in isothermal solidification time. However, during the bonding process, continual interdiffusion of elements between the liquid interlayer and the base metals continually modified the composition of the liquid as solidification progressed. A considerable enrichment of this element in the liquated insert metal during bonding at 1123 and 1223 K could be responsible for the beginning of a solidification regime characterized by a slower isothermal-solidification rate. Besides that, the possible role of the second solute, Cr and Fe, in reducing the isothermal-solidification rates at higher temperatures and the decrease in solubility of Ti with increase in temperature above its eutectic temperature in Zr were important contributing factors. According to Fick's second law of diffusion, and assuming a constant diffusion coefficient:

$$\frac{\partial C}{\partial t} = D\frac{\partial^2 C}{\partial x^2} \tag{1}$$

where $\partial C/\partial t$ is the change in the solute concentration with time at a given position in the base metals, which could provide an indication of isothermal-solidification rate, and D is the diffusion coefficient, and $\partial^2 C/\partial x^2$ is the change in concentration gradient with distance. At any given instant, the concentration gradient ($\partial C/\partial x$) of the diffusing solute in the base metals is influenced by the solute solubility limit and thus $\partial^2 C/\partial x^2$ is also dependent on maximum solute solubility. Therefore, the diffusion-controlled isothermal-solidification rate is not only dependent on diffusion coefficient, but also on solubility, both of which can be influenced differently by the bonding temperature. An increase in the bonding temperature will cause an exponential increase in the solute diffusivity according to the Arrhenius equation. However, according to the Ti–Zr phase diagram the solubility of Ti in Zr decreases with increase in temperature above the eutectic temperature (Fig. 6a). A reduction in the solubility of Ti at the higher temperature could cause a decrease in the rate of change of concentration gradient ($\partial^2 C/\partial x^2$) in the base metals during the bonding operation. This could, according to Fick's second law, reduce Ti diffusion and, as such, decrease the rate of isothermal solidification at the higher temperature. (Fe, Cr)-containing particles were observed within the eutectic products in the joints prepared at the higher temperature where reduction in isothermal-solidification rate with increase in the bonding temperature was observed. The presence of (Fe, Cr)-rich particles within the centreline eutectic, suggests that Fe and Cr diffusion out of liquated interlayer was reduced at the higher bonding temperature.

As stated by Zhou [30] two semi-infinite phases with a coupled diffusion-controlled migrating solid/liquid interface can be considered through the transient liquid phase modelling. The solute concentration can be expressed as

$$C(x,t) = A_1 + A_2\ \mathrm{erf}\left[\frac{x}{\sqrt{4Dt}}\right] \tag{2}$$

where A_1 and A_2 are constants, and the boundary conditions are:

$$C(\infty, t) = C_M$$

$$C(x(t), t) = C_\alpha$$

Likewise, based on the analytical study of transient liquid phase bonding of binary systems, Tuah-Poku et al. [31] developed the following equation to express the dependence of isothermal solidification completion time, $t_{(TLP\text{-}DB)}$, on the bonding temperature:

$$t_{(TLP-DB)} = ((2\pi W_0^2 h)/16D_0) \times \left[(\exp(Q/RT))/(C_{as})^2\right] \tag{3}$$

where W_0 is the initial liquid width, D_0 the diffusion coefficient, Q the activation energy, T the temperature of bonding and $C_{\alpha s}$ is the equilibrium solidus composition of the melting point depressant. They qualitatively showed that, as temperature increases, the time of completing isothermal solidification ($t_{(TLP\text{-}DB)}$) decreases via the exponential term. Nevertheless, an increase in the bonding temperature simultaneously reduces the solidus composition (solid solubility), $C_{\alpha s}$, and, thus, will tend to increase the time required to complete isothermal solidification. This indicates that time, $t_{(TLP\text{-}DB)}$, may not continue to monotonically decrease with increase in temperature but instead will tend to increase as the temperature reaches and exceeds a critical value where the influence of reduced solubility overrides higher diffusivity.

Enrichment of the liquated interlayer with Ti, capable of depressing the melting temperature, may not be responsible for the reduction in isothermal-solidification rate during the bonding process. Interplay between increase in diffusivity and decrease in solubility of melting point depressant Ti with increase in the bonding temperature could be another important factor contributing to the observed reduction in isothermal-solidification rate of the materials. The extent of isothermal solidification during the bonding process depends on the amount of the melting point depressant solute that diffused into the base metals during the hold period. An increase in Ti diffusion into the base alloys with increasing the bonding temperature apparently resulted in a concomitant decrease in the thickness of the residual liquid interlayer that transformed to the centreline eutectic product during cooling.

In another model of the isothermal solidification process mechanism [32,33] the total time for complete isothermal solidification, $t_{f(holding\ time)}$, was estimated:

$$t_f^{0.5} = \frac{2h}{4kD^{0.5}} \tag{4}$$

where k is a dimensionless parameter, h the width of the liquid insert, and D is the diffusion coefficient of the melting point depressants (Ti and Cu) in the solid base alloys, and it is strongly dependent on the bonding temperature through the Arrhenius relationship:

$$D = D_0 \exp\left(-\frac{Q}{RT}\right) \tag{5}$$

where R is the gas constant, T is the absolute bonding temperature and D_0 is the frequency factor. It has been expected that the rate of isothermal solidification rise with increase in the temperature during the bonding operation. However, an increase in the bonding temperature may not necessarily result in a faster solidification process, as the actual rate of solidification will depend upon not only diffusivity but also on solubility of the diffusing solute in the base metals. The dimensionless parameter k can subsequently be determined numerically by the following expression:

$$\Omega = \frac{C_{\alpha L} - C_i}{C_{L\alpha} - C_{\alpha L}} = k\sqrt{\pi}\exp k^{0.5}(1 + \mathrm{erf}(k)) \tag{6}$$

where Ω is a dimensionless thermodynamic parameter (called saturation parameter), C_i is the initial solute concentration in the base metals and the solute concentration in the solid and liquid phase at the interface are $C_{\alpha L}$ and $C_{L\alpha}$, respectively. This equation proves that reducing the bonding time at a particular temperature involves not only selecting melting point depressant with high diffusivity, but also with a high solubility in the base metals and a narrow freezing range. Lesoult [34] used numerical methods to calculate the rate constant k in Eq. (6) and used the value of k to compute the time

required for complete isothermal solidification based on Eq. (7). Increasing k can result in faster solid–liquid interface motion and shorter duration for complete isothermal solidification.

$$t = \frac{W_{\max}^2}{16D} k^{-0.5} \tag{7}$$

where $W_{\max}$ is the maximum width of liquated region obtained during dissolution stage calculated using Eq. (8).

$$W_{\max} = \frac{C_f \cdot W_0}{C_{L\alpha}} \tag{8}$$

Gale and Wallach [13,15] used a different approach to predict $t_{f(\text{holding time})}$ based on the application of Fick's second law of diffusion. They used this approach with the assumption that base metal dissolution and isothermal solidification stage could occur simultaneously instead of sequentially. The solid base material and liquid interlayer were subsequently treated as a continuum where the time required for complete isothermal solidification is

$$C_{\alpha L} - C_i = (C_0 - C_i) \times \operatorname{erf}\left(\frac{w}{\sqrt{4Dt_f}}\right) \tag{9}$$

where C_0 is the initial solute concentration in the interlayer, and w is the initial half thickness of the interlayer. The advantage of this method is that the derived equation can be solved analytically, and its applicability to Zircaloy-4/Ti-base interlayer/stainless steel 321 couple was studied in the present work. Therefore, the total solute amount, m_{Ti}, which has entered the base metal at the bonding time, can be calculated from the following relation:

$$m_{\text{Ti}} = C_{\alpha L}\left(\frac{D_s t}{\pi}\right)^{0.5} \tag{10}$$

and the total amount of the solute diffused into the base metals equals the original solute content of the Ti-base interlayer.

$$C_I w_0 = 2C_{\alpha L}\left(\frac{D_s t}{\pi}\right)^{0.5} \tag{11}$$

where C_I is the solute content in the Ti-base interlayer. It is shown numerically by Jen et al. [35] that the holding time and the holding temperature influence the solute distribution strongly, which in turn influences the diffusion zone thickness. For this case the solute redistribution equation for isothermal solidification can be calculated by

$$C_{\text{solute}} = kC_0\left[1 - \frac{f_s}{1 + \left(\frac{D_s k}{vL}\right)}\right]^{(k-1)} \tag{12}$$

where D_s is the solid-diffusion coefficient at the bonding temperature, L is the isothermally solidified length area, k equilibrium partition ratio equal to C_s/C_L ($C_s = kC_0$), v is growth velocity (cm/s) and f_s is weight fraction of the solid. This equation can prove that Zr of the base metal redistribute to the interlayer because of presenting similar element in the interlayer.

In a new approach Illingworth et al. [36] have developed a new numerical solution scheme based on the Landau transformation and finite-difference equations to solve Fick's second-order differential equation. In their solution the numerical scheme was decoupled into a set of linear equations. The moving boundary has been seen through the solution as a parabolic equation ($s = 2k\sqrt{Dt}$) assuming it conserves the solute during isothermal solidification and k was calculated from Eq. (6). They used a variable spatial discretization and a transient finite difference method to solve the liquid/solid movement interface (Eqs. (13)–(15)).

$$\left[p_i^{j+1}S^{j+1} - p_i^j S^j\right]\left[\frac{u_{i+1} - u_{i-2}}{2}\right] = \frac{\delta t}{S^{j+\sigma}}\left[(D_A)_{i+\frac{1}{2}}^{j+\sigma}\frac{p_{i+1}^{j+\sigma} - p_i^{j+\sigma}}{u_{i+1} - u_i} - (D_A)_{i-\frac{1}{2}}^{j+\sigma}\frac{p_i^{j+\sigma} - p_{i-1}^{j+\sigma}}{u_i - u_{i-1}}\right] + (S^{j+1} - S^j)\left[p_{i+\frac{1}{2}}^{j+\sigma}u_{i+\frac{1}{2}} - p_{i-1/2}^{j+\sigma}u_{i-\frac{1}{2}}\right] \tag{13}$$

$$\left[q_i^{j+1}(L - S^{j+1}) - q_i^j(L - S^j)\right]\left[\frac{v_{i+1} - v_{i-1}}{2}\right] = \frac{\delta t}{L - S^{j+\sigma}}\left[(D_B)_{i+\frac{1}{2}}^{j+\sigma}\frac{q_{i+1}^{j+\sigma} - q_i^{j+\sigma}}{v_{i+1} - v_i} - (D_B)_{i-\frac{1}{2}}^{j+\sigma}\frac{q_i^{j+\sigma} - q_{i-1}^{j+\sigma}}{v_i - v_{i-1}}\right] + (S^{j+1} - S^j)\left[q_{i+\frac{1}{2}}^{j+\sigma}(1 - v_{i+\frac{1}{2}}) - q_{i-\frac{1}{2}}^{j+\sigma}(L - v_{i-\frac{1}{2}})\right] \tag{14}$$

$$\frac{D_B\delta t}{L - S^{j+\sigma}}\left(\frac{q_1^{j+\sigma} - C_B}{v_1}\right) - \frac{D_A\delta t}{S^{j+\sigma}}\left(\frac{C_A - p_{N-2}^{j+\sigma}}{1 - u_{N-2}}\right) = (S^{j+1} - S^j)\left[\frac{1 + u_{N-2}}{2}p_{N-1-\frac{1}{2}}^{j+\sigma} + \frac{1 - u_{N-2}}{2}C_A - \left(1 - \frac{v_1}{2}\right)q_{\frac{1}{2}}^{j+\sigma} - \frac{v_1}{2}C_B\right] \tag{15}$$

where δt is the time step; S^j is the future interface position in time step j; p_i^j is the concentration in phase A (the base metal) in position i in time step j; q_i^j is the concentration in phase B (the filler alloy) in position i in time step j; L is the thickness of phase B plus half-thickness of phase A; u is the proportional position in phase A; C_A is the equilibrium concentration of phase A in contact with B; C_B is the equilibrium concentration of phase B in contact with A; v is the proportional position in phase B; N is the number of discretisation points; D_A is the diffusion coefficient in phase A; D_B is the diffusion coefficient in phase B; σ is a constant between 0 and 1.

In view of the above, an algorithm was solved by writing a program in MATLAB code to simulate the partial transient liquid phase diffusion bonding of the base alloys based on the requirement of conserving the solute. In the algorithm, the intrinsic diffusion coefficients of Ti which is assumed to be diffusion controlling of isothermal solidification process were ($D_{\text{Ti}} = 5.5 \times 10^{-14}\ \text{m}^2\ \text{s}^{-1}$ at the higher bonding temperature and $D_{\text{Ti}} = 9 \times 10^{-14}\ \text{m}^2\ \text{s}^{-1}$ at the lower bonding temperature) greater than those for α-Fe ($D_{\alpha\text{-Fe}} = 5 \times 10^{-15}\ \text{m}^2\text{s}^{-1}$ at the higher bonding temperature), γ-Fe($D_{\gamma\text{-Fe}} = 3 \times 10^{-17}\ \text{m}^2\ \text{s}^{-1}$ at the higher bonding temperature) and Ni ($D_{Ni} = 3 \times 10^{-17}\ \text{m}^2\ \text{s}^{-1}$ at the lower bonding temperature) [37–39]. Thus, diffusion of Ti becomes faster than that of Fe and Ni. However, diffusivity of the melting point depressant solute in the base materials can be calculated using Arrhenius Eq. (5).

The program solves the analytical Eq. (7) numerically using Newton–Raphson method to solve for k efficiently. Input parameters include initial filler thickness W_0, initial concentration of the melting point depressant solute in the filler C_f and in the base metal C_m, solidus and liquidus concentrations of the melting point depressant solute in the base metal, $C_{\alpha L}$ and $C_{L\alpha}$ respectively, and diffusivity of the melting point depressant solute, D, in the base metal. A plot of average eutectic width against square root of holding time is presented in Fig. 7. As can be seen, as the bonding time increases the average eutectic width decreases significantly. In another plot, liquid interlayer half-width against square root of holding time at the different bonding temperature is shown in Fig. 8. It is deduced that at the higher bonding temperature at both sides of the joint width of the liquid interlayer decreases faster than that of used at the lower bonding temperature. Moreover, a derivation from the parabolic law (Eq. (16)) at the higher bonding temperature is observed.

$$x^2 = k_p(t - t_0) \tag{16}$$

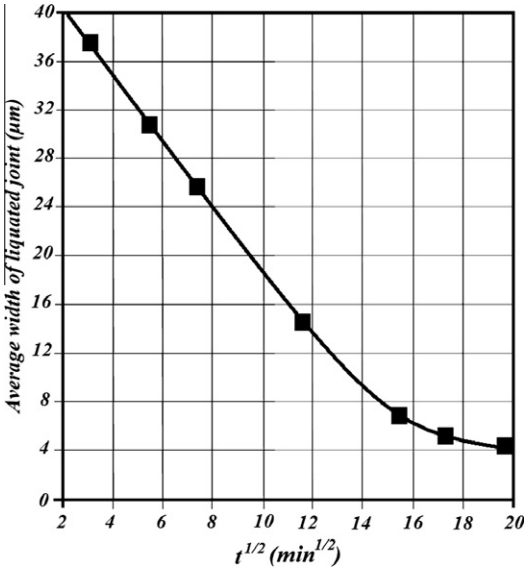

Fig. 7. Plot of average eutectic width versus square root of time.

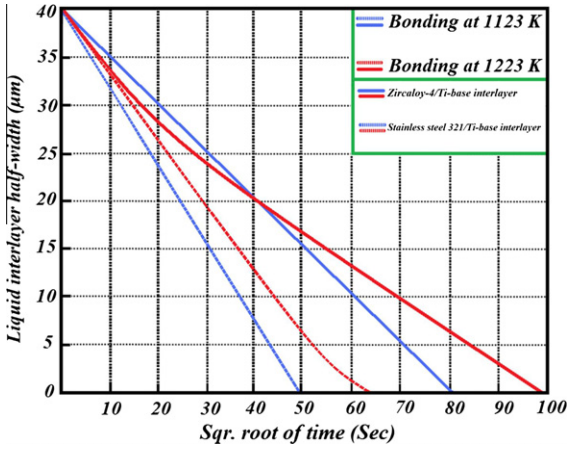

Fig. 8. Numerically simulated variation of half-width of liquated interlayer with square root of time as temperature is increased.

in which x is diffusion distance (μm); k_p is parabolic constant (μm^2/s); t is holding time (s); t_0 is latent period (s) [41]. Observation of this phenomenon in the binary system containing exclusively one melting point depressant solute provides experimental evidence that deviation from the parabolic law is possible under the influence of the concentration gradient of the single diffusing solute without a necessary contribution from the second diffusing melting point depressant solute like Cu. The rate of decrease of the isothermal-solidification rate within the deviation zone, which determines the time required for complete isothermal solidification, is dependent on the magnitude of $(\partial C/\partial x)$ in Eq. (1). The $(\partial C/\partial x)$ is influenced by the solubility of the diffusing solute in the base materials at the bonding temperatures.

3.2.2. Growth of the interlayer during partial transient liquid phase diffusion bonding

Fig. 9 shows the variation of reaction interface (Zircaloy-4/Ti-base interlayer and stainless steel 321/Ti-base interlayer) thickness as a function of the bonding time. It is found that the growth of

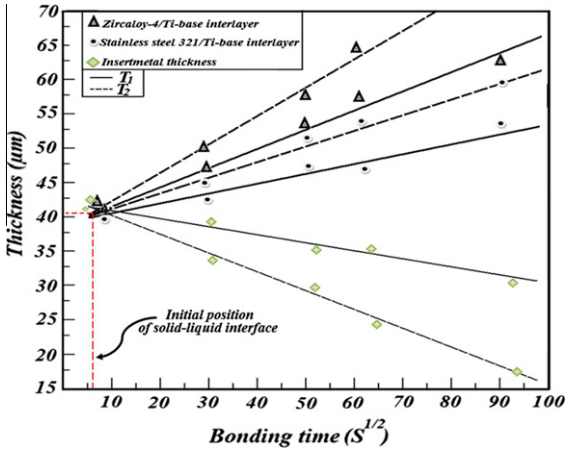

Fig. 9. The effect of bonding time on thickness of reaction layers in two sides of the bonding specimens at T_1 and T_2.

these layers followed the parabolic law and the thickness (x) can be described by

$$x = X + A\sqrt{Dt} \tag{17}$$

where X is the initial interlayer thickness, A is the materials constant, D is the diffusion coefficient, and t is the bonding time. At a definite bonding temperature, D is a constant. Therefore, Eq. (17) can be simplified as

$$x = X + A_g\sqrt{t} \tag{18}$$

where A_g is the reaction layer growth coefficient. After the regression treatment of the experimental data by means of the least square method, the growth coefficients of the reaction interface, in Zircalloy-4 and stainless steel 321 sides were obtained as follows: $A_{g(Ziracaloy\text{-}4/Ti\text{-}base\ \ interlayer)} = 7.21 \times 10^{-6}$ m/s$^{1/2}$ and $A_{g(stainless\ steel\ 321/Ti\text{-}base\ interlayer)} = 1.67 \times 10^{-7}$ m/s$^{1/2}$, respectively. If the A_g results were minus in quantity it was signalled that the interlayer might gradually consumed during the bonding operation, which raised a big question in the hypothetical assumption in terms of taking diffusion coefficient as a constant term. Based upon the above calculations, it is deduced that the interface at the Zircaloy-4/Ti-base interlayer side grew much faster than the interface at the stainless steel 321/Ti-base interlayer side did, owing to the faster diffusion of Ti atoms towards the Zr alloy to react with Zr to form a reaction layer (Fig. 9). For a given bonding time the effect of the bonding temperature on the reaction layers thickness can be described by

$$x^2 = X + A_0 \exp\left(\frac{-Q}{RT}\right)t \tag{19}$$

which after getting logarithm from both sides we have

$$\ln x^2 = -\frac{Q}{RT} + \ln A + \ln X \tag{20}$$

where A_0 is the pre-exponential factor, Q is the activation energy for the growth of the reaction layers at both sides of the joint, R is the universe gas constant, T is the bonding temperature, and A is a constant. The relationship between the reaction layers and the bonding thickness and the bonding temperature is presented in Fig. 10. The reaction layers thickened with increasing the bonding temperature (see Fig. 11). However, the bonding temperature showed much less influence on the reaction layer thickness at the higher bonding temperature. This was due to the low activity of Ti atoms in the Zircaloy-4 side and the slow diffusion of Ti and other components of the interlayer e.g. Ni and Cu towards the stainless steel 321 side. When

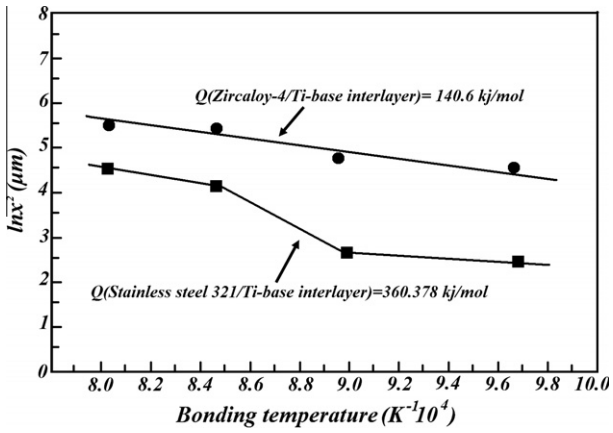

Fig. 10. Effect of the bonding temperature on the growth of reaction layers in Zircaloy4/Ti-base interlayer and stainless steel 321/Ti-base interlayer sides for a constant boning time of 1.2 ks.

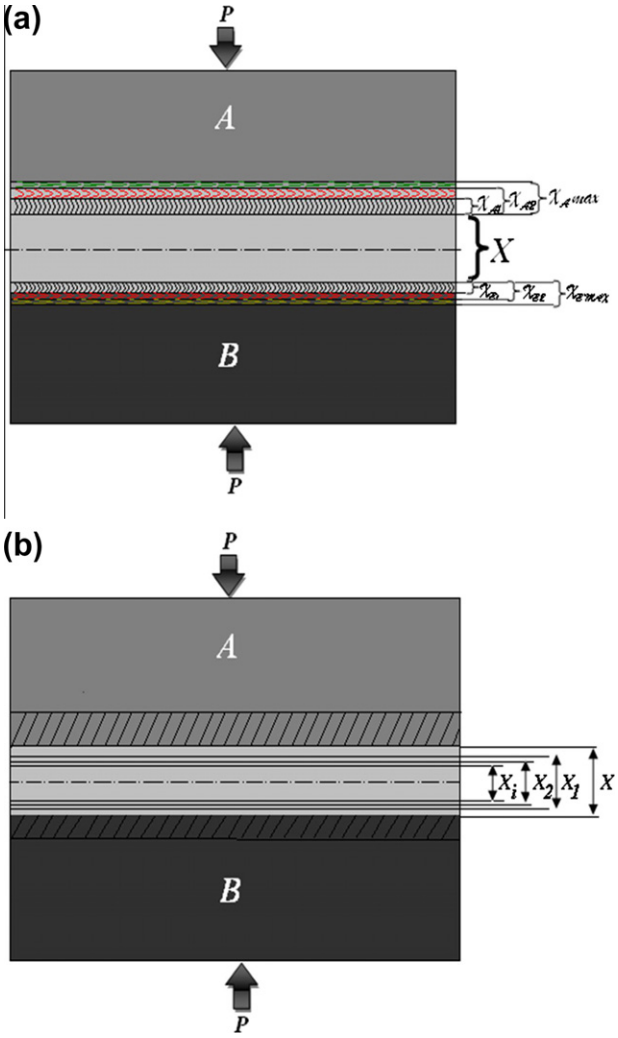

Fig. 11. Schematic illustration of evolution in partial transient liquid phase diffusion bonding of two dissimilar metals using a Ti-base alloy interlayer; (a) thickness evolution of the interlayer in both sides of the bond, (b) thickness evolution of the original interlayer; A: Zircaloy-4 and B: stainless steel. These are pushed towards the final location of the bond line.

the bonding temperature was high enough, the maximum thickness (x_{max}) was observed.

It is obvious that the dissimilar materials have different activation energy and consequently activation energy of the base metals affects the growth of the reaction layers, which can calculate from the slopes of the $\ln x^2$ versus $1/T$ lines. During the bonding operation, the isothermal solidification of the liquid phase leads to the transformation of the interfacial reaction from a solid–liquid reaction to a solid–solid reaction. The further reaction required the migration of the Ti, Ni and Cu toward the reaction layers in both sides. Because the diffusion of the Ti atoms in stainless steel 321 and Zircaloy-4 was in solid state, the corresponding activation energy for the growth of reaction layers was high. In addition, the apparent activation energy for the growth of Ti-base interlayer in the side of stainless steel 321 could also be estimated to be 140.6 kJ/mol from Fig. 10. It is apparent in any system in thermal equilibrium the atoms are constantly colliding with one another and changing their vibrational energy. Therefore, some atoms can lower their free energies when they migrate to other side of the joint. This concentration gradient of the diffusive flux is affected by the gradient of strain energy which can be found when diffusion occurs in the presence of a temperature gradient known as thermomigration. In this investigation, the effect of strain energy is considered in the values of activation energy for the growth of reaction layers. The results obtained show that formation and growth of the reaction layers are simultaneous process, and the growth rates for both the layers follow the parabolic law as shown in Eqs. (18) and (19). Taking logarithm from Eq. (20) yields the time, $t_{(r.l)}$, to form a reaction layer with the thickness, x, and can be rewrite by

$$ln\, t_{r,l} = \frac{Q}{RT} + 2lnx - lnA_0 - lnX \tag{21}$$

The time, $t_{r,l}$, to form the reaction layers can be plotted as a function of temperature as shown in Fig. 12. The time to obtain the certain reaction layer thickness decreases with increase in the temperature. The set of parallel lines with different slopes can be seen in Fig. 12. Given an optimal reaction layer thickness (x_2), the thickness of the Ti-base interlayer can be simultaneously adjusted from X_1 to X_i by changing temperature and time. In this plot an optimal reaction layer thickness (x_2) introduced at relative low temperature for relative long time to obtain thicker reaction layers ($ln\, t_{r,l}$ is the time to form reaction layers and $ln\, t_m$ is the time to form the Ti-base interlayer). It is noticeable that partial transient liquid phase diffusion bonding with longer bonding time is favourable for obtaining thicker interlayer, although the reaction layer can be kept at x_2. In

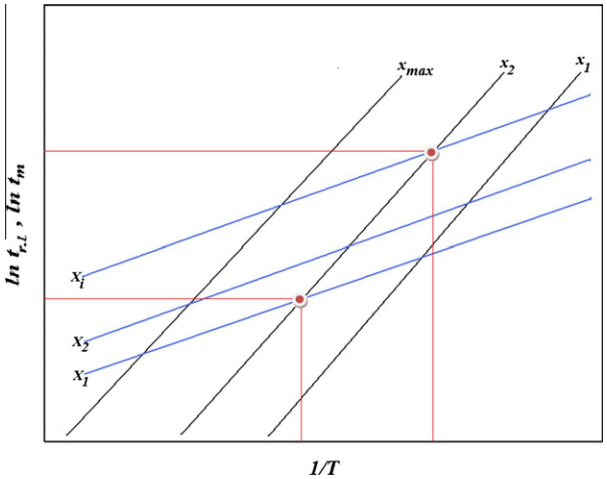

Fig. 12. Controlling the bonding process as a function of the time of reaction layers formation as well as the bonding temperatures.

this plot, however, it can recognize that as the concentration of metals, depending on time, is changed (i.e. in incomplete isothermal solidification), heating and cooling time constantly play a feeble role in widening interdiffusion thickness.

Although the modified solute distribution model is useful to have reasonable estimations of the partial transient liquid phase diffusion bonding time, modified migrating solid/liquid interface model is more reliable and accurate. The results of this study suggest that the present model can be used to predict the optimum condition for the bonding operation of the Zr and Fe alloy systems using Ti-base interlayer in which a large change in concentration occurs.

3.2.3. Formation and growth of intermetallics

The processes of formation and growth of the new phases during diffusion play a significant role in the partial transient liquid phase diffusion bonding of Zircalloy-4 to stainless steel 321 with the Ti alloy filler metal. In the present study, the mechanism and kinetics of formation and growth of the intermetallic phases during the bonding operation are discussed.

Nucleation of the intermetallics in the bonding area relies on deformation of the solid, interdiffusion of the alloying elements and energies supplied. Interdiffusion of the atoms play critical role on the formation of the intermetallic compounds. Atomic properties of the bonding elements significantly influence the interdiffusion of the atoms. From the equilibrium phase diagram, it is known that a lot of intermetallics form when Ti, Fe, Ni and Cr is alloyed with Zr at different ratios [6,12,26]. How two or more metallic atoms mix into each other is determined by Hume-Rothery Rule [42] based upon the variation between their atomic sizes, electro negativity, valence, and crystallinity. The solid state growth of the intermetallic compounds is diffusion controlled. The growth rate is linear with the square root of time at a given temperature and exponential with temperature. In the simplest case of interaction between metal A and metal B, only one intermetallic phase A_mB_n can be formed at the interface. Growth of the intermetallic layer which separating both metals occurs by the advance of at least one of the components toward the interface due to the diffusion. Using Fick's first law yields a parabolic law for intermetallic growth

$$\omega^2 = \frac{2}{Y}(C_B - C_A)D_\omega t_{(I.F)} \tag{22}$$

where ω is the layer thickness, $(C_B - C_A)$ is the difference in concentration at its boundaries, D_ω is the diffusion coefficient of the layer, $t_{(I.F)}$ is the time, and Y is constant which has dimensions of concentration and weakly dependent on the bonding temperature. It should be noted that the diffusion coefficient substantially depends on the real structure of the metals and on the concentration. Consequently, the diffusion flux will depend on the nature and extent of boundaries between grains and also on the temperature, composition and the concentration gradient. It is important to note that intermetallics are growth controlled by the diffusion rate of the fastest diffusing element. Only intermetallics with a range of composition can form. Line compound such as CuTi, Cu_2Ti, $ZrFe_3$ and $(Zr(Fe, Cr)_2)$ will not grow as discrete layers as no diffusion gradient can exist. When there is a solid solubility and diffusion through the intermetallic is constant, the growth rate of the intermetallic is described by the parabolic growth law where the time taken for an intermetallic phase to grow to width ω during isothermal solidification, (t_{IG}), assuming that diffusion into the base metal is negligible, is

$$t_{IG}^{0.5} = \omega\sqrt{\frac{\rho_s}{D(C_\omega - C_0)}} \tag{23}$$

where ρ_s refers to the solid density and C_ω is the intermetallic composition and a mass balance on the liquid interlayer to the intermetallic given by

$$\omega = \frac{W_i C_i}{C_{aic}} \tag{24}$$

where C_{aic} is the average intermetallic composition, W_i is the width of the interlayer and C_i is the initial interlayer composition. For example an estimated diffusion constant of 5×10^{-10} cm^2/s was rapid enough to form Cu-rich intermetallics. In this case an estimate of the diffusivity of Ti into the Zr alloy at the bonding temperatures can be obtained using the relation $D = x^2/t$. It is convincible that the effect of the bonding temperature on the isothermal solidification time is high enough to let the diffused elements form a new intermetallic compound. As the bonding temperature increased, the overall composition of the joint sensitively changed from Ti-rich to Zr-rich owing to the different reactivity of Zr in the filler with the Ti and Zr in the base metals. Fig. 5 shows the compositional change of the main phases in the joints at 1123 K, which is plotted on a Ti–Zr–Cu ternary liquid projection. It shows that with increasing the bonding time, Ti-rich phases can be formed and after 20 min the joint turn to have a Zr-rich phase. Such a different composition in the joints could be explained by a different degree of a dissolution or diffusion of the Ti and Zr base metals into the joint. Becker [43] found that the rate of the formation of the new intermetallic phase is

$$V_{in} = \mathscr{R}\exp\left(-\frac{E}{RT_b}\right)\exp\left(-\frac{I_{cr.n}}{RT_b}\right) \tag{25}$$

where $\mathscr{R}$ is constant, E the activation energy of the diffused atoms and $I_{cr.n}$ is the energy of forming a critical nucleus. The time of formation of a nuclei of the intermetalic, t_{in} also is vigorously depends on the temperature of the bonding process

$$t_{in} = \mathscr{R}'\exp\left(\frac{I_{cr.n} + E}{RT_b}\right) \tag{26}$$

where $\mathscr{R}'$ is a constant, T_b is the bonding temperature and $I_{cr.n}$ can be calculated by

$$I_{cr.n} = \frac{\phi}{2} \times \frac{\gamma^2 V^2}{\Delta\mu} \tag{27}$$

where ϕ is the shape factor, γ is the specific free surface energy of the nucleus, V is the atomic volume and $\Delta\mu$ is the difference in chemical potentials of atoms in the original lattice and in the nucleus. The width of the different intermetallic phases has been also measured by the cursor position during the characterization of the interface in SEM. Average of the intermetallic width has been given in Fig. 13 and is compared with the presented analytical model. Individual phase width (ω_{ex}) varies with the bonding temperature. Assuming the growth of each phase to be parabolic, the width can be determined from the expression

$$\omega_{ex} = H\sqrt[n]{t} \times \exp\left(\frac{Q}{RT}\right) \tag{28}$$

and

$$H = H_0\exp\left(\frac{Q}{RT}\right)\ \mathrm{m\ s^{-1/2}} \tag{29}$$

where H is the interdiffusion rate constant, t the time of diffusion in seconds, Q the activation energy for layer growth in kJ mol^{-1} and $n = 2$ for parabolic growth of the individual phases [44]. Value of Q is estimated for the intermetallics with considering the plot of $ln\,\omega_{ex}$ versus $1/T$. Nonetheless, it should be pointed out that the accuracy of the analytical model predictions is profoundly dependent upon the accuracy of relevant chemical diffusion data. When

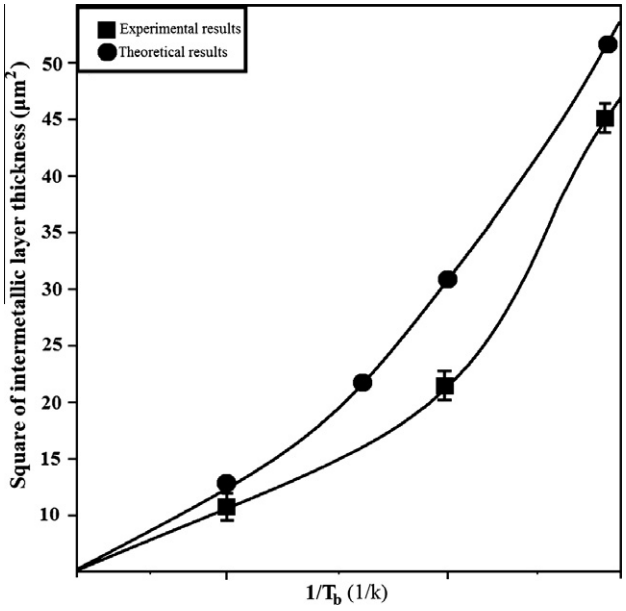

Fig. 13. Effect of the bonding temperature on the intermetallic thickness.

reliable data are available, the bonding kinetics given by the present models are useful in developing partial transient liquid phase diffusion bonding process parameters.

4. Conclusions

In this study, the microstructural evolution of the Zircaloy-4/stainless steel 321 couple was comprehensively investigated when using an active Ti-base interlayer. The important findings are as follows.

(1) Zircaloy-4 has successfully joined to stainless steel 321 by partial transient liquid phase diffusion bonding at the temperatures 1123 and 1223 K, using an active Ti alloy interlayer. Joining was accompanied by the formation of diffusion zones, the thickness of which increased with temperature and structural changes on the Zircalloy-4 side.

(2) As the bonding temperature increased, the overall composition of the joints changed from Ti-rich to (Ti–Cu)-rich, and finally into Zr-rich. Such a different composition in the joints was caused by the different degree of the interatomic diffusion reaction of the Ti as a main element in the filler with the Zr and Fe as the base metals. The ratios between Ti, Cu, Zr, Fe, and Cr were close to CuTi, Cu_2Ti, $ZrFe_3$ and $ZrFe_2$ phases. Lave intermetallic ($Zr(Fe, Cr)_2$) was also observed in the diffusion zone.

(3) Based on the observed compositional variations and phase morphologies of each joint, it was deduced that microstructures of all joints were mainly involved in the isothermal solidification and thereafter the solid-state atomic interdiffusion during the isothermal holding.

(4) The migration of the solute has been numerically modelled using a fully implicit conservative finite difference scheme derived by Illingworth et al. [36]. The results showed a derivation from the parabolic law at the higher bonding temperature. This deviation is caused by reduction in the solute concentration gradient below a critical value due to continual diffusion of the melting point depressant solute from the liquated interlayer into the base materials during holding at the bonding temperature.

(5) The model proposed for the partial transient liquid phase diffusion bonding is in good agreement with the experimental results for boundary displacement. Depending on the new approach, it was shown that a more realistic final bonding time could be predicted for Zircaloy-4/Ti-base interlayer/Stainless steel 321 bonds considering the evolution of the interlayer during the bonding operation.

(6) Average of the intermetallic width during the bonding compared with the analytical model showed that increasing the bonding temperature considerably affect the nucleation and width of the new intermetallics.

References

[1] T. Hirabayashi, T. Sato, C. Sagawa, N.M. Masaki, M. Saeki, T. Adachi, Journal of Nuclear Materials 174 (1990) 45–52.
[2] A.I.A. Almarshad, A.C. Klein, Journal of Nuclear Materials 183 (2) (1991) 186–194.
[3] J. Senevat, P. Mainy, Journal of Nuclear Materials 178 (1991) 315–320.
[4] A. Ravi Shankar, S. Suresh Babu, Mohammed Ashfaq, U. Kamachi Mudali, K. Prasad Rao, N. Saibaba, A. Baldev Raj, Journal of Materials Engineering and Performance 18 (9) (2009) 1272–1279.
[5] J.I. Akhter, M. Ahmad, G. Ali, Materials Characterization (2008), doi:10.1016/j.matchar.2008.08.009.
[6] M. Ghosh, K. Bhanumurthy, G.B. Kale, J. Krishnan, S. Chatterjee, Journal of Nuclear Materials 322 (2003) 235–241.
[7] Zhou Hairong, Zhou Bangxin, Journal of Nuclear Power Engineering, 1997-01.
[8] W.A. Owczarski, Journal of Welding 41 (1962) 78–83.
[9] M. Ahmad, J.I. Akhter, Q. Zaman, M.A. Shaikh, M. Akhtar, M. Iqbal, E. Ahmed, Journal of Nuclear Materials 317 (2003) 212–216.
[10] K. Bhanumurthy, J. Krishnan, G.B. Kale, R.K. Fotedar, A.R. Biswas, Journal of Materials Processing Technology 54 (1995) 322–325.
[11] V. Kalin, V. Fedotov, O. Sevryukov, A. Plyuschev, I. Mazul, A. Gervash, R. Giniatulin, Journal of Nuclear Materials 271&272 (1999) 410–414.
[12] H.I. Shaaban, F.H. Hammad, Journal of Nuclear Materials 78 (2) (1978) 431–433.
[13] M.L. Wayman, R.R. Smith, M.G. Wright, Metallurgical Transactions A 17A (1986) 429–434.
[14] G.B. Kale, K. Bhanumurthy, K.C. Ratnakala, S.K. Khera, Journal of Nuclear Materials 138 (1986) 73–80.
[15] J.I. Akhter, M. Ahmad, M. Iqbal, M. Akhtar, M.A. Shaikh, Journal of Alloys and Compounds 399 (2005) 96–100.
[16] A.A. Shirzadi, E.R. Wallach, Acta Materialia 47 (13) (1999) 3551–3560.
[17] W.D. MacDonald, T.W. Eager, Annual Review of Materials Science 22 (1992) 23–46.
[18] C. Lemaignan, A.T. Motta, in: R.W. Cahn, P. Haasen, E.J. Kramer (Eds.), Nuclear Materials, in: B.R.T. Frost (Ed.), Materials Science and Technology, vol. 10B, VCH, Weinheim, Germany, 1994, p. 1 (Chapter 7).
[19] A. Miquet, D. Charquet, C. Michaut, C.H. Allibert, Journal of Nuclear Materials 105 (1982) 142–148.
[20] N.V. Bangaru, R.A. Busch, J.H. Schemel, in: R. Adamson, L. van Swam (Eds.), Zirconium in the Nuclear Industry: Seventh International Symposium, vol. ASTM STP 939, American Society for Testing and Materials, Philadelphia, USA, 1987, p. 341.
[21] G. Ökvist, K. Källström, Journal of Nuclear Materials 35 (1970) 316.
[22] R. Arroyave, T.W. Eagar, L. Kaufman, Journal of Alloys and Compounds 351 (2003) 158–170.
[23] S.J. Lee, S.K. Wu, R.Y. Lin, Acta Materialia 46 (1998) 1297–1305.
[24] H.I. Shaaban, F.H. Hammad, Journal of Nuclear Materials 71 (1978) 277–285.
[25] Y. Nakao, Transactions of Japan Welding Society 20 (1) (1989) 60–65.
[26] Y. Zhou, W.F. Gale, T.H. North, International Materials Reviews 40 (5) (1995) 181–196.
[27] O.A. Ojo, N.L. Richards, M.C. Charturvedi, Science and Technology of Welding and Joining 9 (2004) 532–540.
[28] C.W. Sinclair, Journal of Phase Equilibria 20 (4) (1999) 361–369.
[29] C.W. Sinclair, G.R. Purdy, J.E. Morral, Metallurgical Transactions A 31A (2000) 1187–1192.
[30] Y. Zhou, Journal of Materials Science Letters 20 (2001) 841.
[31] I. Tuah-Poku, M. Dollar, T.B. Massalski, Metallurgical Transactions A 19A (1988) 675–686.
[32] A. Sakamoto, C. Fujiwara, T. Hattori, S. Sakai, Welding Journal 68 (1989) 63.
[33] J.E. Ramirez, S. Liu, Welding Journal 71 (1992) 365s.
[34] G. Lesoult, Centre for Joining of Materials Report, Carnegie Mellon University, Pittsburgh, PA, 1976.
[35] Tien-Chien Jen, Yuning Jiao, Numerical Heat Transfer, Part A: Applications 39 (2) (2001) 123–138.
[36] T.C. Illingworth, I.O. Golosnoy, Journal of Computational Physics 209 (2005) 207–225.
[37] B. Aleman, I. Guitterrez, J.J. Urcola, Materials Science and Technology 9 (1993) 633–641.

[38] M. Ghosh, S. Kundu, S. Chatterjee, B. Mishra, Materials Transactions 36A (2005) 1891–1899.
[39] S. Hinotani, Y. Ohmari, Transactions, Japan Institute of Metals 29 (1988) 116–124.
[40] A. Sakamoto, C. Fujiwara, T. Hattori, S. Sakai, Welding Journal 68 (4) (1989) 63–71.
[41] Wang Juan, Li Yajiang, Ma Haijun, Vacuum 80 (2) (2006) 426–431.
[42] W. Moffatt, G. Pearsall, J. Wulff, Structure and Properties of Materials 1 (1971).
[43] R. Becker, Annals of Physics 32 (1938) 128–140 (in German).
[44] G.B. Kale, R.V. Patil, P.S. Gawde, Journal of Nuclear Materials 257 (1998) 44–50.